Characterization of the concentration of agar-based soft tissue mimicking phantoms by impact analysis

Anne-Sophie Poudrel, Arthur Bouffandeau, Oriane Le Demeet, Giuseppe Rosi, Vu-Hieu Nguyen, Guillaume Haiat

Characterization of the concentration of agar-based soft tissue mimicking phantoms by impact analysis

Anne-Sophie Poudrel[1], Arthur Bouffandeau[1], Oriane Le Demeet[1], Giuseppe Rosi[2], Vu-Hieu Nguyen[2], and Guillaume Haiat*[1]

[1]CNRS, Univ Paris Est Creteil, Univ Gustave Eiffel, UMR 8208, MSME, F-94010 Créteil, France

[2]Univ Paris Est Creteil, Univ Gustave Eiffel, CNRS, UMR 8208, MSME, F-94010 Créteil, France

Abstract

In various medical fields, a change of soft tissue stiffness is associated with its physio-pathological evolution. While elastography is extensively employed to assess soft tissue stiffness *in vivo*, its application requires a complex and expensive technology. The aim of this study is to determine whether an easy-to-use method based on impact analysis can be employed to determine the concentration of agar-based soft tissue mimicking phantoms. Impact analysis was performed on soft tissue mimicking phantoms made of agar gel with a mass concentration ranging from 1% to 5%. An indicator Δt is derived from the temporal variation of the impact force signal between the hammer and a small beam in contact with the sample. The results show a non-linear decrease of Δt as a function of the agar concentration (and thus of the sample stiffness). The value of Δt provides an estimation of the agar concentration with an error of 0.11%. This sensitivity of the impact analysis based method to the agar concentration is of the same order of magnitude than results obtained with elastography techniques. This study opens new paths towards the development of impact analysis for a fast, easy and relatively inexpensive clinical evaluation of soft tissue elastic properties.

Keywords Soft tissues, Impact analysis, Elastic properties, Agar-based phantom, Elastography

*Corresponding author : guillaume.haiat@cnrs.fr

1 Introduction

In various medical and surgical fields such as oncology, hepatology, plastic surgery or dermatology, the assessment of elastic properties of soft tissues is of great importance for clinical diagnostic and patient follow-up, since the development of many pathological processes is associated with an alteration of the tissue mechanical properties and changes in tissue stiffness (1; 2). Tumorous or fibrous tissues are typically characterized by an elastic modulus that differs from surrounding healthy tissues by several orders of magnitude (3; 4). In dermatology too, many skin diseases as scleroderma, Ehlers-Danlos or keloids induce alterations of the mechanical properties of the skin, which can be assessed by measuring, for instance, the elastic properties of the tissue (5). Due to these manifold clinical issues, the quantitative and non-invasive characterization of soft tissues mechanical properties is of great medical interest.

Palpation is an empirical method commonly used by the physicians in order to inspect tissue stiffness and detect tissue abnormalities. However, this method remains subjective. Quantitative methods such as quasi-static compression tests, nano-indentation or dynamic measurements such as rheometry or Dynamic Mechanical Analysis (DMA) are widely used to characterize material elastic or viscoelastic properties. However, their destructive nature as well as reproducibility issues prevent such approach to be used in the clinic and they can only be employed for *in vitro* tests.

Interestingly, elastography, whose development started in the 1990's (6), has been extensively used to characterize soft tissue stiffness by mapping the tissue compressive and shear moduli in different anatomical locations, as it can be applied *in vivo*. In particular, transient elastography, which relies on shear wave propagation, remains one of the gold standard for clinical evaluation of local tissue Young's modulus (7; 8). A medical device named Fibroscan® is now commonly used for the assessment of hepatic fibrosis (9). However, the use of shear-waves requires a complex and relatively expensive system, which may limit the use of the technology. In dermatology, although elastography has also been investigated (5), another simpler method based on skin suction and consecutive deformation has been developed for skin elasticity assessment, for which the corresponding medical device is known as Cutometer® (10; 11). This instrument may be used to assess skin aging (12) and the efficiency of cosmetic treatments (10; 13). However, this method is based on empiric observations and suffers from reproducibility issues (13). Moreover, it remains difficult to analyse the different parameters obtained with the Cutometer® and to retrieve the actual viscoelastic properties of the skin (10).

In the context of total hip arthroplasty, our group has developed a technique based on impact analysis aiming at providing information on the stability of the acetabular cup implant (14; 15; 16) and of the femoral stem (17; 18; 19). This technique is based on the analysis of the signal corresponding to the variation of the force as a function of time obtained during an impact between the ancillary holding the implant and an instrumented hammer equipped with a force sensor. More recently, the method was extended to be applied to osteotomy procedures (20; 21) and in particular rhinoplasty (22; 23; 24). The analysis of the impact force signal between the instrumented hammer and the osteotome proved to be able to estimate the bone properties (elastic modulus and thickness) (20) as well as to predict the rupture of bone samples (21). In these specific

configurations (22; 24; 23), impact analysis was directly performed on the osteotome whose cutting end was a linear contact with the bone tissue. The main advantages of our approach lies in the fact that i) it is easy to use (i.e. fast and simple measurement protocols), ii) it provides a real-time feedback, iii) it is non-invasive and non-destructive, iv) it is a dynamic measurement, portable and low cost. In particular, the method sensitivity to the biologic tissue properties as well as the non-invasive and non-destructive characteristics of the method makes it relevant to be applied to various clinical applications from dermatology and cosmetology to oncology.

The aim of this paper is to determine whether an easy-to-use method based on impact analysis can be employed to determine the concentration of agar-based soft tissue mimicking phantoms. Impact analyses are performed with soft tissue mimicking phantoms made of agar, a biological polymer. Agar-based phantoms have been extensively employed to mimic biological soft tissues (25; 26; 27), since they have similar mechanical properties with adjustable concentration-dependent mechanical characteristics (28; 29; 30; 31). A signal processing technique similar to the one developed in Hubert et al. (20) is employed to evaluate the method sensitivity to variations of the agar concentration. The non linear behavior of the experimental configuration is assessed by applying preloading conditions. Eventually, the sensitivity of the method is compared to DMA and elastography techniques using results obtained in the literature. The originality of this study is to apply impact force analysis to soft matter, with a rigidity of around three orders of magnitude lower than the bone tissue considered in the previous study on bone characterization (20), [1], which required to adapt the experimental setup. The maximum amplitude of the force is ten times lower in the present work than in Hubert et al. (20). Another difference between the present work and the work described in (20; 21) lies in the targeted clinical application. While bone characterization and bone rupture detection were considered in (20; 21) the overall objective of the present study is to eventually distinguish healthy and pathological soft tissues.

2 Materials and methods

2.1 Preparation of tissue mimicking phantoms

Tissue mimicking phantoms were made by varying the concentration of agar from 1g to 5g in 100ml of distilled water, leading to samples with agar concentration c in weight of 1%, 2%, 3%, 4% and 5%, respectively. Samples above 5% were not tested due to the brittle nature of agar at higher concentrations. A picture of the samples is shown in Fig. 1 for each concentration c. The ingredients were mixed at room temperature and then the solution was heated in a microwave oven up to the boiling point following the protocol employed in Manickam et al. (32) to ensure the homogeneity of the samples. The solution was left at room temperature until it reached 50°C and it was poured into a cylinder mould. The samples were cylinders with an height and a diameter equal to 20 mm. Three samples were prepared from the same solution and then analyzed for each concentration c.

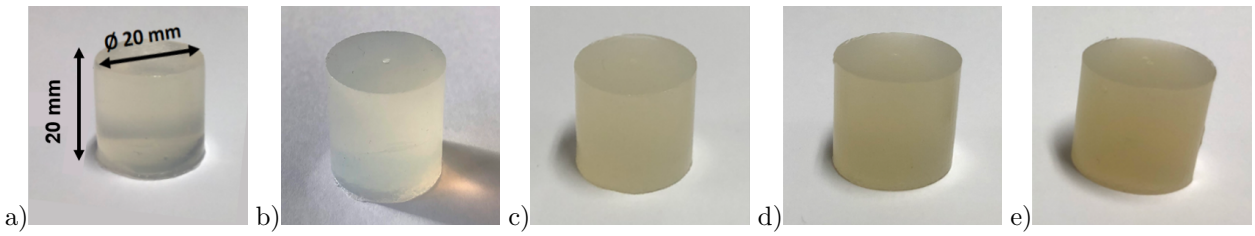

Figure 1: Pictures and dimensions of the soft tissue mimicking phantoms made of agar concentration $c = 1\%$ (a), $c = 2\%$ (b), $c = 3\%$ (c), $c = 4\%$ (d) and $c = 5\%$ (e).

2.2 Impact measurements

2.2.1 Experimental set-up

A description of the set-up device used for impact measurements is shown in Fig. 2. The experimental set-up was composed of a small instrumented hammer of 5g (8204, Brüel and Kjaer, Naerum, Denmark) with a sensitivity of 22.7 mV/N and a cylindrical beam positioned in a guiding support, so that the beam was kept vertical and perpendicular to the phantom sample during the testing procedure. The custom-made aluminum beam used, named "*AlD1*", had a length of 80 mm and a diameter of 4 mm, with one extremity of 1 mm diameter.

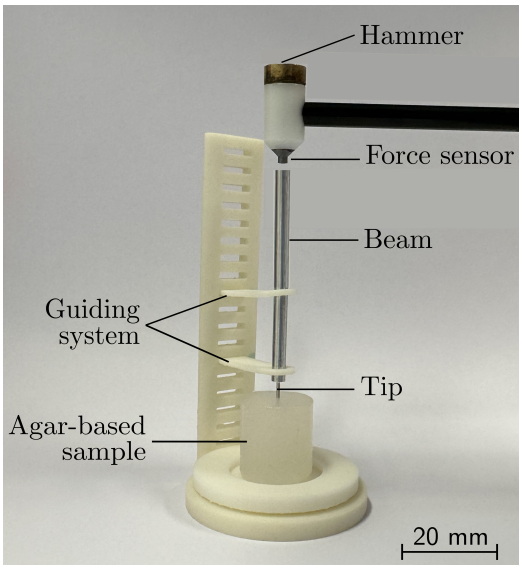

Figure 2: Illustration of the experimental set-up used for impact measurements on agar-based samples.

For the tests in preloading conditions only, five stainless steel cylindrical masses of 10.9 g, 21.6 g, 32.7 g, 43.8 g and 54.9 g with an external diameter of 20 mm were successively put on the agar-based sample of each concentrations c, from the lightest to the heaviest. A 5 mm diameter hole was machined in the center of the cylinders to allow *AlD4* to be in contact with the agar-based samples for impact measurements under preloading conditions. Impact tests were performed for each mass and each agar concentration.

2.2.2 Experimental protocol

The force signal $s_i(t)$ corresponding to each impact $\#i$ was recorded by the force sensor located on the impact face of the hammer. The signal was acquired in Labview interface (National Instruments, Austin, TX, USA) with a data acquisition module of 51.2 kHz sampling frequency (NI 9234, National Instruments, Austin, TX, USA). The measurement procedure consisted in applying four impacts on the upper surface of the beam with the hammer shown in Fig. 2. Only impacts for which the maximum value of $s_i(t)$ was comprised between 1N and 10N were considered, which will be discussed in the Section 4.

2.3 Analysis of the impact force signal

A dedicated signal processing method was implemented and adapted from Hubert et al. (20) in order to analyze the signals $s_i(t)$. An example of a typical force signal $s_i(t)$ is shown in Fig. 3. For each signal $s_i(t)$, the two first maxima were considered, which correspond to i) the impact of the hammer on the beam and ii) the rebound of the beam on the hammer following the impact. The amplitude of the first peak of the force signal $s_i(t)$ was noted A_i and will be named as the impact force in what follows.

A temporal indicator, noted Δt and given in ms, was calculated as the average over the four impacts $\#i$ of the time difference Δt_i between the first and second local maxima of the signal $s_i(t)$, following:

$$\Delta t = \frac{1}{4}\sum_{i=1}^{4} \Delta t_i, \qquad \Delta t_i = t_{i,2} - t_{i,1} \tag{1}$$

where $t_{i,1}$ and $t_{i,2}$ correspond to the time of the first and second local maxima of the signal $s_i(t)$, respectively.

Note that the 3^{rd} and 4^{th} peaks correspond to the 2^{nd} and 3^{rd} rebounds of the beam on the hammer, respectively, and are not considered in the following impact analysis.

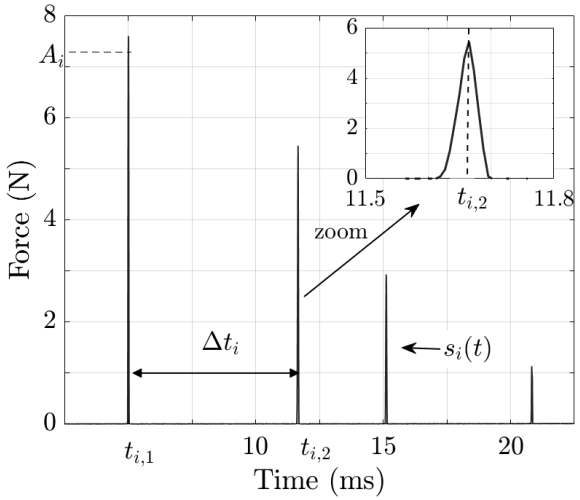

Figure 3: Illustration of a signal $s_i(t)$ corresponding to the variation of the impact force as a function of time obtained for a given impact on sample #1 with agar concentration $c = 2\%$ and zoom on the second peak at $t_{i,2}$.

The reproducibility of the impact measurement method was assessed by repeating three times the measurement of Δt on each sample of each agar concentration c. The corresponding mean value $\overline{\Delta t}$ and the standard

deviation $\sigma_{\Delta t}$ were calculated. $\sigma_{\Delta t}$ was defined as the intra-sample variability and corresponds to the method reproducibility. Moreover, the standard deviation associated to the variation of $\overline{\Delta t}$ over three samples of the same agar concentration, noted $\Sigma_{\Delta t}$, was also calculated for each agar concentration and represents the inter-sample variability.

3 Results

The values of the time indicators $\overline{\Delta t}$, calculated from the impact force signals $s_i(t)$ are given in Table 1 for each sample and each agar concentration c comprised between 1% and 5%. The intra-sample variability, $\sigma_{\Delta t}$, is of the same order of magnitude than the inter-sample variability $\Sigma_{\Delta t}$ (except for $c = 1\%$). The intra-sample variability $\sigma_{\Delta t}$, is slightly higher for the agar concentration $c = 1\%$ ($\sigma_{\Delta t} \sim 5\%$) than for the others ($\sigma_{\Delta t} < 2\%$).

The indicator $\overline{\Delta t}$ decreases as a function of the agar concentration c (see Table 1). An example of the variation of $\overline{\Delta t}$ is shown in Fig. 4 for measurements performed on the sample #1 of each concentration c. An ANOVA analysis was performed on the values of Δt for all samples. The results confirm that the values of Δt are significantly different between each agar concentration c (p-value=7.10^{-41}).

In what follows, only the standard deviation related to the reproducibility of the method, that is the intra-sample variability $\sigma_{\Delta t}$, will be considered in order to focus on the performances of the impact measurement method and not on the reproducibility of the procedure used to produce the agar sample.

	1%			2%			3%			4%			5%		
Sample	#1	#2	#3	#1	#2	#3	#1	#2	#3	#1	#2	#3	#1	#2	#3
$\overline{\Delta t}$ (ms)	9.99	9.80	9.88	6.62	6.74	6.72	5.53	5.50	5.52	5.05	5.01	5.02	4.50	4.52	4.55
$\sigma_{\Delta t}$ (ms)	0.50	0.33	0.49	0.05	0.13	0.13	0.01	0.03	0.07	0.07	0.03	0.02	0.04	0.02	0.07
$\Sigma_{\Delta t}$ (ms)		0.09			0.07			0.01			0.02			0.02	

Table 1: Values of the time indicators $\overline{\Delta t}$ calculated from the impact force signals $s_i(t)$ measured on each sample of each agar concentration c between 1% and 5%. The intra-sample variability $\sigma_{\Delta t}$ and the inter-sample variability $\Sigma_{\Delta t}$ are also indicated. All the values are given in millisecond.

The variation of the temporal indicator $\overline{\Delta t}$ as a function of the preload is shown in Fig. 5 for measurements performed on the sample #1 for each agar concentration c between 1% and 5%. For each value of c, the indicator $\overline{\Delta t}$ decreases when the preload value increases. A linear regression analysis, represented by the dotted lines in Fig. 5, is performed between the values of $\overline{\Delta t}$ and the values of the preload, for each agar concentration c. The values of the slope a and the correlation coefficient R^2 obtained from the linear regression analysis are given in Table 2 for the three sets of samples. A significant linear relation is obtained with a correlation coefficient R^2 higher than 0.60 for all the agar concentrations. The decrease of $\overline{\Delta t}$ as a function of the preload is higher for smaller agar concentrations (see Fig. 5). In particular, the slope of the linear regression curves varies from $a = -2.6$ ms/% to $a = -0.33$ ms/% in average over the three samples between $c = 1\%$ and $c = 5\%$ (see Table 2).

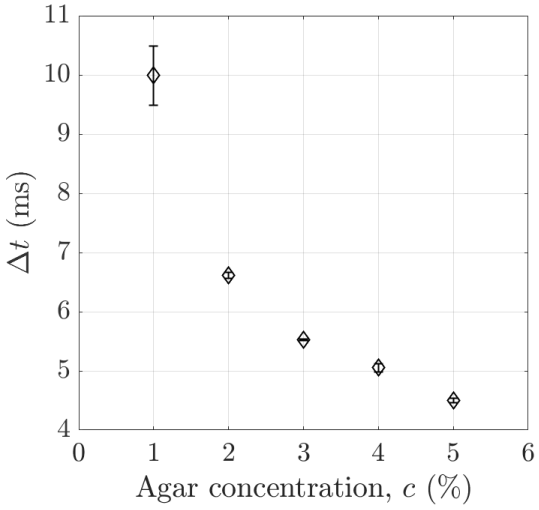

Figure 4: Variation of the time indicator $\overline{\Delta}t$ as a function of the agar concentration c between 1% and 5% for measurements performed on the sample #1 for each concentration. The error bars correspond to the intra-sample variability, $\sigma_{\Delta t}$.

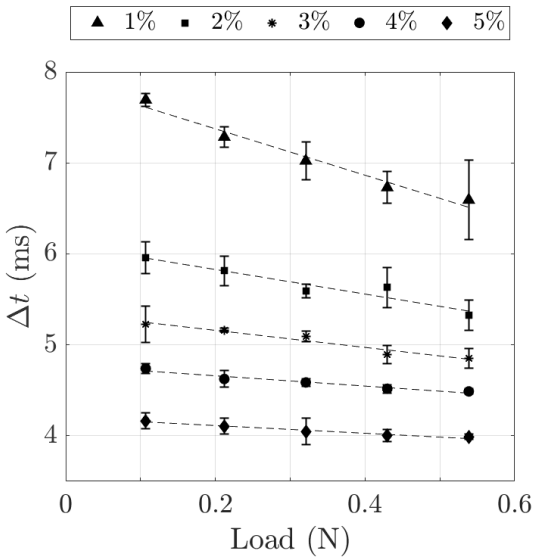

Figure 5: Variation of the time indicator $\overline{\Delta}t$ as a function of the preload applied on the sample #1 made of agar concentration c between 1% and 5%. The dotted lines represent the linear regression analysis. The error bars correspond to the intra-sample variability, $\sigma_{\Delta t}$.

	1%			2%			3%			4%			5%		
Sample	#1	#2	#3	#1	#2	#3	#1	#2	#3	#1	#2	#3	#1	#2	#3
a	-2.5	-2.3	-3.1	-1.3	-1.8	-1.7	-0.9	-0.6	-0.4	-0.5	-0.2	-0.7	-0.4	-0.2	-0.4
R^2	0.97	0.97	0.98	0.91	0.77	0.97	0.95	0.94	0.91	0.94	0.60	0.97	0.95	0.97	0.87

Table 2: Values of the slope a and the correlation coefficient R^2 obtained from the linear regression analysis of the values of $\overline{\Delta}t$ as a function of the preload for each set of sample and each agar concentration c between 1% and 5%.

4 Discussion

The main purpose of the present study was to investigate the feasibility of using impact analysis to distinguish soft tissue mimicking phantoms with different agar concentration and to evaluate the sensitivity of the technique

with regard to the agar concentration, which is known to be highly dependent on the sample stiffness (33; 34; 32). Impact analysis, which has been successfully employed by our group to evaluate the bone elastic modulus (20), the bone-implant stiffness (14; 15; 17; 19; 18), and to predict bone fracture (21) is applied herein to characterize agar-based samples. The main advantages of the proposed impact method compared to other dynamic techniques such as elastography are: i) the simple set-up and measurement protocol and ii) its relative inexpensive nature.

4.1 Physical interpretation

The temporal indicator Δt is shown to decrease as a function of the agar concentration (see Fig. 4). This phenomenon may be explained by an increase of the sample stiffness when the agar concentration increases, which has been widely demonstrated in the literature using various quasi-static (33; 34; 32; 35) and dynamic characterisation techniques (28; 36). Quasi-static compression tests under small deformations showed in particular that the elastic modulus of agar-based sample of concentrations from 0.5% to 3% in weight varies between 7kPa to 200kPa (33). Note that this range of elastic moduli covers values of healthy and abnormal human soft tissues stiffnesses (3). Interestingly, Nayar et al. (34) performed dynamic indent tests at a frequency of 100 Hz and reported values of viscoelastic dissipation $\tan(\delta)$ between 0.01 and 0.06 for agar concentrations between 5% and 0.5% respectively. The decrease of the temporal indicator Δt with the increase of the sample stiffness is coherent with results found in previous studies on the evaluation of biomechanical properties of bone tissues using impact analysis (20; 24). In Hubert et al. (20), similar impact measurements were performed on bone mimicking phantoms and on plywood samples using an osteotome. The samples considered in Hubert et al. (20) had very different material stiffness, but could also be distinguished based on a time indicator equivalent to Δt in the present study, that was lower for the higher stiffnesses. The relation between the temporal indicator Δt and the agar-based sample stiffness is also consistent with previous studies that used impact analysis to evaluate bone-implant system stiffness (17; 19; 18). Both in experimental (17; 19; 18) and numerical studies (16), it was observed that the higher the bone-implant system stiffness, the shorter the time between the two first peaks of the impact force signal, which may be explained by an increase of the resonance frequency of the system when the sample stiffness increases.

The temporal indicator Δt is shown to decrease when the value of the preload applied to the sample increases (see Fig. 5). The influence of the preload on the value of Δt may be explained by the non-linear elastic behavior of the agar material, which has been established in the literature (33; 7; 30; 37). In Manickam et al. (32), the shear modulus was measured with and without compression of the samples, similarly to what was done in the present work for impact measurements with preloading conditions. The value of the shear modulus increased with the compression applied to the samples (32), which is consistent with the results shown in Fig. 5, where Δt (inversely proportional to the sample stiffness) decreases when the value of the preload increases for all concentration of agar in the range [1-5]%. However, for a same value of the preload, the strain is higher for smaller agar concentrations. For example, for $c = 1\%$, the highest preload correspond to a strain of 8% while

it represents only 1% when $c = 5\%$. Therefore, the results obtained in Fig. 5 and Table 2 do not provide a direct relationship between the agar concentration and the non-linearity of the material sample since the level of strains is not equivalent between the agar concentrations. Note that in Pavan et al. (37), it was shown that the non-linearity of the stress-strain curves of agar/gelatin mixture did not depend on agar concentrations in the range $0.58\% \leq c \leq 2.81\%$.

This method can be compared with the approach described in Kontiola (38), where the authors used an electromechanical method to measure intraocular pressure. A probe was conceived to collide with the eye surface and to bounce back on it. However, the method was different from the present paper because an acceleration sensor was used to measure the duration of contact.

4.2 Analytical model

In order to better understand the response of the system to the impact of the hammer on the beam, a simple 1-D model described schematically in Fig. 6 was developed. This model was adapted from the one described in Hubert et al. (20) and takes into account the mechanical and geometrical properties of the set-up.

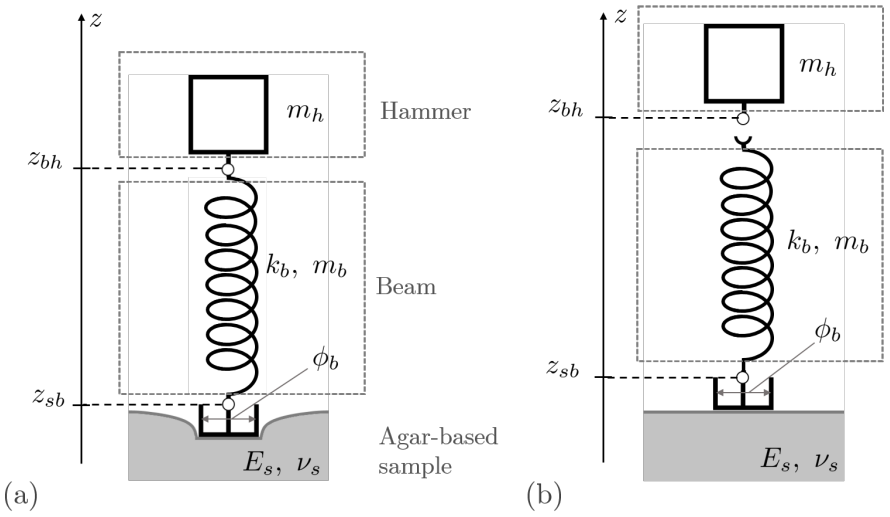

Figure 6: Schematic representation of the 1-D analytical model of the experimental set-up: (a) the hammer is in contact with the beam and (b) the hammer is not in contact with the beam.

First, the hammer was assimilated to a point mass m_h and the beam was modeled by a mass-spring system with a mass m_b and a stiffness k_b given by:

$$m_b = \rho_b \, \pi \, L_b \, (\phi_b/2)^2 \tag{2}$$

$$k_b = \frac{E_b \, \pi \, (\phi_b/2)^2}{L_b} \ , \tag{3}$$

where E_b is the Young's modulus and ν_b is the Poisson's ratio of the beam, ρ_b is its mass density, L_b is its length and ϕ_b its section diameter. The phantom sample was considered to be an isotropic elastic half-space characterized by the Young's modulus E_s, which is the only free parameter of the model, and a constant

Poisson's ratio $\nu_s = 0.5$. Note that we did not consider a viscoelastic behaviour for the bone sample because it would lead to a very complex model of the flat punch contact, as described in Popov et al. (39). The coordinates along the vertical $z-$direction of the sample/beam and beam/hammer contacts were denoted by z_{sb} and z_{bh} respectively. While the contact interaction between the hammer and the beam was considered as punctual, the contact interaction between the sample and the beam was described as a frictionless indentation of a flat-ended cylindrical punch against an isotropic elastic half-space (40; 41). Based on the previous assumptions, an analytical model governed by a system of two coupled equations could be derived:

$$\begin{cases} m_b \ddot{z}_{sb} = k_b \left(z_{bh} - z_{sb} - L_b \right) - \phi_b E^* z_{sb} \\ m_h \ddot{z}_{bh} = -k_b \left(z_{bh} - z_{sb} - L_b \right) \end{cases} \tag{4}$$

$$\begin{cases} m_b \ddot{z}_{sb} = -\phi_b E^* z_{sb} \\ m_h \ddot{z}_{bh} = 0 \end{cases}, \tag{5}$$

with $E^* = \dfrac{1}{\dfrac{(1-\nu_s^2)}{E_s} + \dfrac{(1-\nu_b^2)}{E_b}}$.

Equation 4 corresponds to the case where the hammer is in contact with the beam (*i.e.* $z_{bh} - z_{sb} = 0$) and Equation 5 corresponds to the case where there is no contact between the hammer and the beam (*i.e.* when $z_{bh} - z_{sb} > L_b$). For a given impact velocity of the hammer v_i, corresponding to the initial condition, the system of Eqs. 4 and 5 were solved using the Runge-Kutta 4^{th} order method (42) and the software Matlab (The Mathworks, Natick, MA, USA).

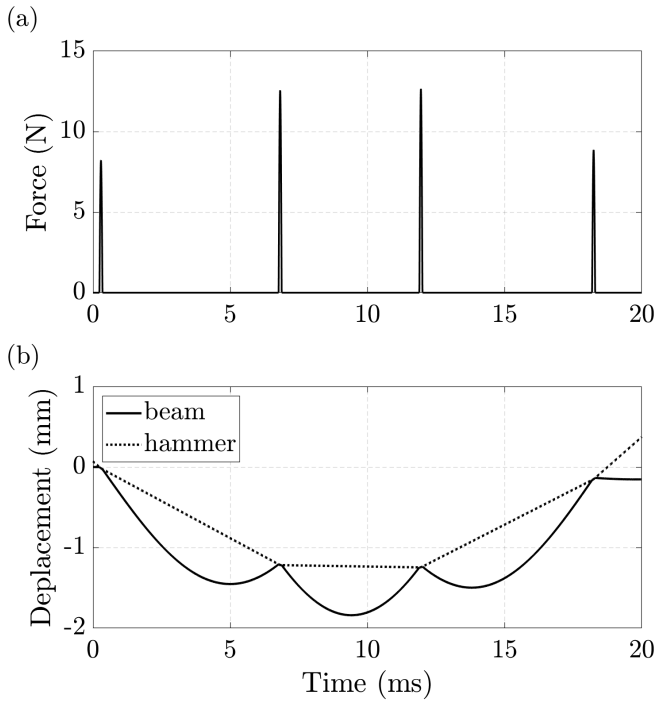

Figure 7: Variation of (a) the force signal and (b) the displacements of the elements (hammer and beam) as a function of time obtained with the 1-D model using the "AlD1" aluminum beam and a sample with stiffness $E_s = 100$ kPa.

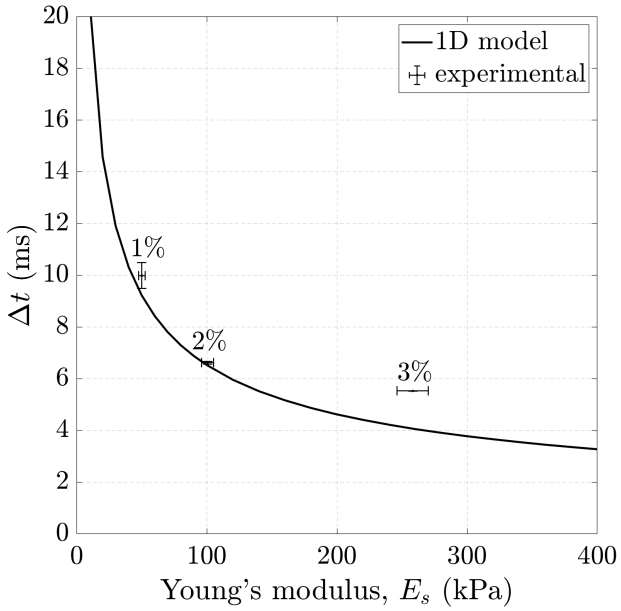

Figure 8: Variation of (a) the force signal and (b) the displacements of the elements (hammer and beam) as a function of time obtained with the 1-D model using the "AlD1" aluminum beam and a sample with stiffness $E_s = 100$ kPa.

Figure 7 shows the variation of the force as a function of time during an impact considering a hammer with a mass of 5g, an "AlD1" aluminum beam and a sample with a Young's modulus $E_s = 100$ kPa. The analytical results are qualitatively similar to the experimental ones (see Fig. 3). The variation of the indicator Δt as a function of the Young's modulus of the sample obtained with this 1-D model is shown in Fig. 8. The analytical results are in the same order of magnitude as the experimental ones derived from the values of Young's moduli reported in the literature (see Table 4), except for a slight underestimation of Δt for an agar concentration of 3%. However, the characteristics of agar hydrogels are very sensitive to the preparation and storage conditions and to the measurement method. For example, for an agar gel at a given concentration, their elastic properties can vary by one or two orders of magnitude (43).

This simple 1D analytical model is useful to understand the general behavior of the indicator Δt regarding the geometric or mechanical parameters of the system such as E_s, the Young's modulus of the sample. However, the slight differences with the experimental results may be explained by several reasons. First, despite the dynamic nature of impact analysis, a quasi-static modeling of the flat-ended cylindrical punch was considered. Second, the use of this flat-punch model does not take into account the friction and adhesion phenomena that can occur at the contact. Third, the choice of an isotropic elastic half-space for the tissue mimicking phantoms neglects the viscoelastic phenomena and the potential boundary conditions induced by the sample geometry. Fourth, the actual properties of the agar samples were not measured and values taken from the literature were used instead. Despite these limitations, a good agreement between analytical and experimental results was obtained.

4.3 Sensitivity analysis

The sensitivity of the impact method (including the measurements and analyses) to determine the agar concentration c of a sample is analyzed by a simple two steps method described in what follows (refer to (44; 45)

for more details). The first step is to perform a linear regression analysis of the average value of the temporal indicator Δt as a function of the agar concentration c based on the results shown in Table 1 and Figure 4. The linear regression analysis is performed for each set of sample (#1, #2, #3) leading to:

$$\tilde{\Delta t} = a \times c + b \tag{6}$$

where $\tilde{\Delta t}$ is the approximate value of Δt and (a, b) are the coefficients obtained from the linear regression analysis of the variation of Δt as a function of the agar concentration c in the range $c \in$[1-5]%.

The second step of the method consists in assessing the error realized by the impact method on the estimation of the agar concentration c, noted in what follows c_{err} (expressed in % of agar). To do so, the averaged measurement reproducibility error, σ_m, corresponding to the mean value of the intra-sample variability $\sigma_{\Delta t}$ in the range $c \in$[1-5]% is calculated for each set of sample (#1, #2, #3). The error c_{err} is evaluated by combining σ_m with the linear regression analysis in Eq. 6) following:

$$c_{err} = |\sigma_m / a| \tag{7}$$

Table 3 shows the results obtained for the error c_{err} on the estimation of the agar concentration using the impact method. These values of c_{err} are of the same order of magnitude than results obtained from other dynamic characterization methods used *in vivo*, such as elastography or *in vitro*, such as DMA (Dynamic Measurement Analysis) (see Table 4). Based on studies obtained from the literature (35; 46; 47), the error on the agar concentration estimation with Magnetic Resonance Elastography (MRE) (35; 46) or Optical Coherence Elastography (OCE) (47) is close to 0.07 % of agar, which is almost twice the value obtained with DMA (46). Note that the values of error were calculated using the two steps method described above and the elastic moduli and the standard deviations indicated in Table 4 obtained for the different methods and the different agar concentrations c (35; 46; 47).

Set of sample	a (ms/%)	b (ms)	R^2	σ_m (in ms)	c_{err} (% of agar)
#1	-1.25	10.1	0.82	0.14	0.11
#2	-1.23	10.0	0.84	0.11	0.09
#3	-1.24	10.0	0.84	0.16	0.13

Table 3: Results of the linear regression analysis (slope a and intercept b), averaged standard deviation σ_m of Δt in the range $c \in$[1-5]%, and error c_{err} realized on the estimation of the agar concentration in the range $c \in$[1-5]% for each set of sample.

4.4 Influence of the impact force

In this study, the maximum amplitude A_i of the impact force applied with the beam *AlD1* was chosen so that $A_i \in$ [1-10] N because i) higher amplitudes would have drilled the sample, especially for the small agar concentrations and ii) lower amplitude do not allow to produce a sufficient level of energy to retrieve valuable information. Moreover, the values of Δt may vary with the impact force A_i, which limits the extent of the force interval range. A second beam, named "*AlD4*", with a length of 40 mm and a diameter of 4 mm was used

Agar concentration c (%)	Young's modulus E (kPa) MRE (35)	MRE (46)	OCE (47)	DMA (46)	Dissipation tan (δ) DMA (34)
0.5	13.5±0.6	-	-	-	0.06
1	50.1±2.5	-	25.0 ± 2.2	-	0.02
1.5	105.6±6.0	52.3± 3.4	49.7±4.9	42.8±4	-
2	171.4±22.8	100.6±4.7	116.1 ±12.1	75.1±0.6	0.01
2.5	-	157.1±6.8	-	147.8±4.1	-
3	-	258.2±12.1	-	242.4±4.7	-
3.5	-	324.3±26.7	-	324.9±13.1	-
5	-	-	-	-	0.01
Error c_{err} (% of agar)	0.08	0.08	0.07	0.04	-

Table 4: Values of Young's moduli E (given in kPa) and viscoelastic dissipation tan(δ) reported in the literature for different agar concentrations c and measured with elastography in (35; 46; 47) and DMA in (46; 34). The values of the error c_{err} on the estimation of the agar concentration c are calculated for the different techniques. The signs "-" indicate that the measurements were not reported by the authors for these agar concentrations.

to study the influence of the impact force on the results. *AlD4* allows to apply higher forces without drilling the sample. Figure 9 shows the influence of the impact force A_i in the range [1-40] N obtained with *AlD4* on the values of Δt for agar concentrations c between 1% and 5%. The results confirm the dependence of Δt on A_i, which indicates that the measurements should be performed in a reduced force interval for A_i, in order to limit the variations due to the influence of the impact force on Δt. In particular, Δt decreases as a function of the impact force A_i for all the agar concentrations, until reaching a threshold at $A_i \sim 30$N (see Fig. 9). The variation of Δt with regard to the impact force A_i is higher for the smaller agar concentrations. Note that in previous studies on bone stiffness evaluation (20) or implant stability assessment by impact analysis (17; 19; 18), Δt was not shown to depend on the impact force.

Different phenomena may explain the behavior of Δt with regard to the impact force observed herein. A change of the dynamic impact force amplitude affects both the amplitude and the strain rate experienced by the sample (37). Assuming that Δt is related to the sample stiffness, the variation of the dynamic amplitude of the impact force may therefore lead to non-linear effects on Δt due to the three following distinct but coupled phenomena: i) the viscoelastic behavior of the sample (34; 26; 32; 27), ii) the non-linearity of the contact (here flat punch conditions) between the sample and the beam, and iii) the elastic non-linearity of the material.

Note that the impact force can easily be determined for each impact, so that impacts taken into account in a measurement can easily be selected based on the value of A_i, which leads to a minimization of the variability due to this parameter.

4.5 Limitations and perspectives

This study has several limitations. First, the standard deviation $\sigma_{\Delta t}$ (estimated in Table 1) related to the determination of Δt comes from different phenomena. The first one may come from the experimental setup. The value of Δt may be influenced by the orientation of the beam with regard to the surface of the sample. Thereby, the device should be improved in order to guarantee the beam vertical alignment and its perpendicularity with the surface of the sample to be tested, while minimizing the friction in the guiding system (see Fig. 2) and at the beam/sample interface. Moreover, the flatness of the tested face of the sample has not been quantified,

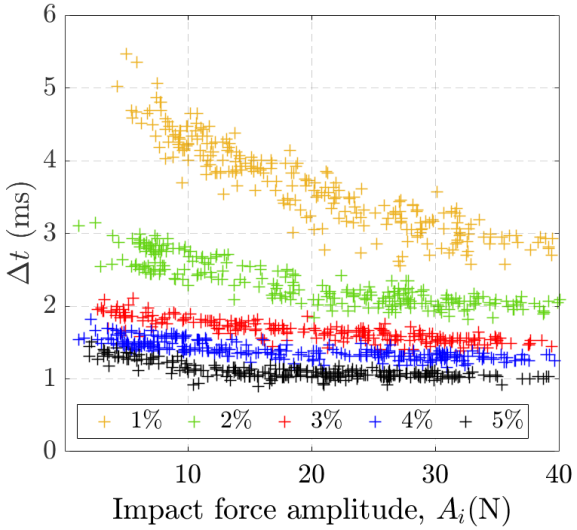

Figure 9: Variation of the values of Δt_i as a function of the impact force A_i in the range [0-40] N for agar concentrations c between 1% and 5%. The measurements were performed with the beam AlD4. Note that each point corresponds to one impact $\#i$.

although it may also influence the system alignment. The second cause of error is the temporal resolution of the measurement of 0.02 ms, which is of the same order of the standard deviation $\sigma_{\Delta t}$.

Second, further works need to be realized to comfort our approach. In particular, analytical and/or numerical modeling is needed to understand the relation between the sample elastic properties and the values of the indicator Δt, similarly as what was done by Hubert et al. (20) for rigid tissues. Such a model could also be useful to investigate the effect of various experimental parameters on the measurement, such as the beam mechanical and geometrical characteristics as well as the sample geometry. In particular, based on a simple flat punch model (41) in the static regime, we expect that the diameter of the beam should be determine the size (in terms of thickness and radius) of the region of interest of the phantom that is measured with our method. Therefore, all the measurements were carried out using with the same beam and with samples with the same dimensions. Moreover, it was verified experimentally that the value of Δt was not significantly modified for samples with larger diameter and larger height than the dimensions considered herein, which was the criteria used to choose the sample dimensions. In addition, it was verified that the results were not influenced by the position of the beam on the sample surface with regard to the boundary conditions.

Third, the sensitivity analyses evaluate the sensitivity of the quantities measured by the different methods (impact analysis, DMA, elastography) with regard to the agar concentration. Such analysis was a first step to validate the feasibility of impact analysis to distinguish materials with different stiffness values, since the influence of the agar concentration on the sample rigidity is well known in the literature. The next step will be to evaluate the sensitivity of impact analysis to the Young's Modulus by performing compression tests.

Fourth, the quality of the soft tissue mimicking phantoms should be improved to obtain a mechanical behavior closer to the one of biological soft tissues. The performances of the method should be tested with more dissipative samples for which the viscoelastic properties strongly vary according to strain rate. Since a change of the impact force amplitude could lead to a change of the strain rate, it is thus expected that the method will

be more sensitive to the force amplitude than what was obtained in Fig. 9. Moreover, it could be relevant to develop heterogeneous samples, and to test the sensitivity of the impact method to the presence of an inclusion (30; 48; 49). Although agar-based phantoms are widely used to mimic soft tissue properties (28; 36; 50; 33; 34), *in vitro* experiments should be carried out on biological living tissues in order to be closer to a future clinical application. A first approach could be to perform tests on muscles, liver or skin, which are among the most important applications targeted by the impact method for living tissue elastic properties evaluation.

An interesting perspective would be to determine the method resolution (both axial and lateral) to detect tissue heterogeneities. As indicated above, based on classical contact mechanics (41), we expect that this resolution is of the order of magnitude to the beam diameter. Another perspective would be to develop a decision-support system to be used in the clinic in order to simply and rapidly determine the local properties of soft tissues. To do so, it will be necessary to control the reproducibility of the measurements and to allow a simple positioning of the beam compared to the targeted tissue. In the present work, the beam was always oriented vertically so that its axis remains perpendicular to the sample surface to guarantee the same contact conditions between the sample and the beam. If oriented with an angle, the surface of the beam in contact with the sample would change, which would lead to a modification of the rigidity of the system and hence to a change of the value of Δt. Moreover, the results would also be likely to change if the beam was not vertically aligned because of the influence of the beam weight on the results. However, considering a non-vertical orientation of the beam could possibly allow to perform similar measurements, which would need to be verified experimentally in a future study. The advantage of the approach is that it is very cheap (only a force sensor is needed) and that it is instantaneous. However, further validations *ex vivo*, *in vivo* and then in a clinical environment are necessary.

5 Conclusion

The present study deals with the elastic characterization of soft tissue mimicking phantoms by impact analysis. To do so, agar-based samples of different concentrations were tested and the sensitivity of the method to determine the agar concentration, related to the sample stiffness, was analyzed. The method consists in applying several impacts on the samples *via* a metallic beam using an instrumented hammer. The temporal signal of the impact force is analysed in real-time. Based on previous studies on the evaluation of bone biomechanical properties by impact analysis, a time indicator Δt is derived from the force signal, corresponding to the time difference between the impact and the rebound of the beam on the hammer. The indicator Δt is shown to decrease when the agar concentration increases, which corresponds to an increase of the sample stiffness. The sensitivity of the impact method to estimate the agar concentration from the value of the indicator Δt is of the same order of magnitude compared to other quantitative methods used *in vivo* such as transient elastography. The impact method presents the advantages to be non-invasive, to provide real-time information and to be relatively inexpensive and easy to use. However, to confirm the potential of impact analysis for *in*

vivo evaluation of soft tissue elastic properties, further investigations must be carried out with biological tissues.

6 Funding

This project has received funding from the European Research Council (ERC) under the European Union's Horizon 2020 research and innovation program (grant agreement No 682001, project ERC Consolidator Grant 2015 BoneImplant), from the project OrthAncil (ANR-21-CE19-0035-03) and from the project OrthoMat (ANR-21-CE17-0004).

7 Declaration of Conflicting Interests

The authors declare that they have no financial or non-financial interests that are directly or indirectly related to the work submitted for publication.

References

[1] Skovoroda AR, Klishko AN, Gusakyan DA, Mayevskii YI, Yermilova VD, Oranskaya GA, et al. Quantitative analysis of the mechanical characteristics of pathologically changed soft biological tissues. Biophysics. 1995;6(40):1359-64.

[2] Andoh F, Yue JL, Julea F, Tardieu M, Noûs C, Pagé G, et al. Multifrequency magnetic resonance elastography for elasticity quantitation and optimal tissue discrimination: A two-platform liver fibrosis mimicking phantom study. NMR in biomedicine. 2021 Aug;34(8):e4543.

[3] Krouskop TA, Wheeler TM, Kallel F, Garra BS, Hall T. Elastic Moduli of Breast and Prostate Tissues under Compression. Ultrasonic Imaging. 1998 Oct;20(4):260-74.

[4] Wells PNT, Liang HD. Medical ultrasound: imaging of soft tissue strain and elasticity. Journal of The Royal Society Interface. 2011 Nov;8(64):1521-49.

[5] Gennisson JL, Baldeweck T, Tanter M, Catheline S, Fink M, Sandrin L, et al. Assessment of elastic parameters of human skin using dynamic elastography. IEEE Transactions on Ultrasonics, Ferroelectrics, and Frequency Control. 2004 Aug;51(8):980-9.

[6] Ophir J, Céspedes I, Ponnekanti H, Yazdi Y, Li X. Elastography: a quantitative method for imaging the elasticity of biological tissues. Ultrasonic Imaging. 1991 Apr;13(2):111-34.

[7] Catheline S, Gennisson JL, Fink M. Measurement of elastic nonlinearity of soft solid with transient elastography. The Journal of the Acoustical Society of America. 2003 Dec;114(6):3087-91.

[8] Bercoff J, Chaffai S, Tanter M, Sandrin L, Catheline S, Fink M, et al. In vivo breast tumor detection using transient elastography. Ultrasound in Medicine & Biology. 2003 Oct;29(10):1387-96.

[9] Sandrin L, Fourquet B, Hasquenoph JM, Yon S, Fournier C, Mal F, et al. Transient elastography: a new noninvasive method for assessment of hepatic fibrosis. Ultrasound in Medicine & Biology. 2003 Dec;29(12):1705-13.

[10] Dobrev H. Use of Cutometer to assess epidermal hydration. Skin Research and Technology. 2000;6(4):239-44.

[11] Bonaparte JP, Ellis D, Chung J. The effect of probe to skin contact force on Cutometer MPA 580 measurements. Journal of Medical Engineering & Technology. 2013 Apr;37(3):208-12.

[12] Ahn S, Kim S, Lee H, Moon S, Chang I. Correlation between a Cutometer® and quantitative evaluation using Moire topography in age-related skin elasticity. Skin Research and Technology. 2007;13(3):280-4.

[13] Stroumza N, Bosc R, Hersant B, Hermeziu O, Meningaud JP. Intérêt du cutomètre pour l'évaluation de l'efficacité des traitements cutanés en chirurgie plastique et maxillo-faciale. Revue de Stomatologie, de Chirurgie Maxillo-faciale et de Chirurgie Orale. 2015 Apr;116(2):77-81.

[14] Michel A, Bosc R, Vayron R, Haiat G. In Vitro Evaluation of the Acetabular Cup Primary Stability by Impact Analysis. Journal of Biomechanical Engineering. 2015 Mar;137(3):031011.

[15] Michel A, Bosc R, Meningaud JP, Hernigou P, Haiat G. Assessing the Acetabular Cup Implant Primary Stability by Impact Analyses: A Cadaveric Study. PLOS ONE. 2016 Nov;11(11):e0166778.

[16] Michel A, Nguyen VH, Bosc R, Vayron R, Hernigou P, Naili S, et al. Finite element model of the impaction of a press-fitted acetabular cup. Medical & Biological Engineering & Computing. 2017 May;55(5):781-91.

[17] Tijou A, Rosi G, Vayron R, Lomami HA, Hernigou P, Flouzat-Lachaniette CH, et al. Monitoring cementless femoral stem insertion by impact analyses: An in vitro study. Journal of the Mechanical Behavior of Biomedical Materials. 2018 Dec;88:102-8.

[18] Albini Lomami H, Damour C, Rosi G, Poudrel AS, Dubory A, Flouzat-Lachaniette CH, et al. Ex vivo estimation of cementless femoral stem stability using an instrumented hammer. Clinical Biomechanics. 2020 Jun;76:105006.

[19] Dubory A, Rosi G, Tijou A, Lomami HA, Flouzat-Lachaniette CH, Haïat G. A cadaveric validation of a method based on impact analysis to monitor the femoral stem insertion. Journal of the Mechanical Behavior of Biomedical Materials. 2019 Nov;103:103535.

[20] Hubert A, Rosi G, Bosc R, Haïat G. Using an Impact Hammer to Estimate Elastic Modulus and Thickness of a Sample During an Osteotomy. Journal of Biomechanical Engineering. 2020 Feb.

[21] Bas Dit Nugues M, Rosi G, Hériveaux Y, Haïat G. Using an Instrumented Hammer to Predict the Rupture of Bone Samples Subject to an Osteotomy. Sensors (Basel, Switzerland). 2023 Feb;23(4):2304.

[22] Lamassoure L, Giunta J, Rosi G, Poudrel AS, Bosc R, Haïat G. Use of an instrumented hammer as a decision support system during rhinoplasty: validation on an animal model. Computer Methods in Biomechanics and Biomedical Engineering. 2020 Nov;23.

[23] Lamassoure L, Giunta J, Rosi G, Poudrel AS, Meningaud JP, Bosc R, et al. Anatomical subject validation of an instrumented hammer using machine learning for the classification of osteotomy fracture in rhinoplasty. Medical Engineering & Physics. 2021 Sep;95:111-6.

[24] Lamassoure L, Giunta J, Rosi G, Poudrel AS, Bosc R, Haiat G. Using an Impact Hammer to Perform Biomechanical Measurements during Osteotomies: Study of an Animal Model. Proceedings of the Institution of Mechanical Engineers Part H, Journal of engineering in medicine. 2021 Apr;235:9544119211011824.

[25] Culjat MO, Goldenberg D, Tewari P, Singh RS. A review of tissue substitutes for ultrasound imaging. Ultrasound in Medicine & Biology. 2010 Jun;36(6):861-73.

[26] Maccabi A, Shin A, Namiri NK, Bajwa N, St John M, Taylor ZD, et al. Quantitative characterization of viscoelastic behavior in tissue-mimicking phantoms and ex vivo animal tissues. PloS One. 2018;13(1):e0191919.

[27] Catheline S, Gennisson JL, Delon G, Fink M, Sinkus R, Abouelkaram S, et al. Measurement of viscoelastic properties of homogeneous soft solid using transient elastography: An inverse problem approach. The Journal of the Acoustical Society of America. 2004 Dec;116(6):3734-41.

[28] Normand V, Lootens DL, Amici E, Plucknett KP, Aymard P. New insight into agarose gel mechanical properties. Biomacromolecules. 2000;1(4):730-8.

[29] Ebenstein DM, Pruitt LA. Nanoindentation of soft hydrated materials for application to vascular tissues. Journal of Biomedical Materials Research Part A. 2004;69A(2):222-32.

[30] Madsen EL, Hobson MA, Shi H, Varghese T, Frank GR. Tissue-mimicking agar/gelatin materials for use in heterogeneous elastography phantoms. Physics in Medicine and Biology. 2005 Nov;50(23):5597-618.

[31] Dahmani J, Laporte C, Pereira D, Bélanger P, Petit Y. Predictive Model for Designing Soft-Tissue Mimicking Ultrasound Phantoms With Adjustable Elasticity. IEEE Transactions on Ultrasonics, Ferroelectrics, and Frequency Control. 2020 Apr;67(4):715-26.

[32] Manickam K, Machireddy RR, Seshadri S. Characterization of biomechanical properties of agar based tissue mimicking phantoms for ultrasound stiffness imaging techniques. Journal of the Mechanical Behavior of Biomedical Materials. 2014 Jul;35:132-43.

[33] Hall TJ, Bilgen M, Insana MF, Krouskop TA. Phantom materials for elastography. IEEE Transactions on Ultrasonics, Ferroelectrics, and Frequency Control. 1997 Nov;44(6):1355-65.

[34] Nayar VT, Weiland JD, Nelson CS, Hodge AM. Elastic and viscoelastic characterization of agar. Journal of the Mechanical Behavior of Biomedical Materials. 2012 Mar;7:60-8.

[35] Hamhaber U, Grieshaber Fa, Nagel Jh, Klose U. Comparison of quantitative shear wave MR-elastography with mechanical compression tests. Magnetic Resonance in Medicine. 2003;49(1):71-7.

[36] McIlvain G, Ganji E, Cooper C, Killian ML, Ogunnaike BA, Johnson CL. Reliable Preparation of Agarose Phantoms for Use in Quantitative Magnetic Resonance Elastography. Journal of the mechanical behavior of biomedical materials. 2019 Sep;97:65-73.

[37] Pavan TZ, Madsen EL, Frank GR, Adilton O Carneiro A, Hall TJ. Nonlinear elastic behavior of phantom materials for elastography. Physics in Medicine and Biology. 2010 May;55(9):2679-92.

[38] Kontiola A. A new electromechanical method for measuring intraocular pressure. Documenta Ophthalmologica Advances in Ophthalmology. 1996;93(3):265-76.

[39] Popov VL, Heß M, Willert E. Handbook of Contact Mechanics: Exact Solutions of Axisymmetric Contact Problems. Springer Nature; 2019.

[40] Sneddon IN. The relation between load and penetration in the axisymmetric boussinesq problem for a punch of arbitrary profile. International Journal of Engineering Science. 1965 May;3(1):47-57.

[41] Johnson KL. Contact Mechanics. Cambridge: Cambridge University Press; 1985.

[42] Runge–Kutta Methods. In: Numerical Methods for Ordinary Differential Equations. John Wiley & Sons, Ltd; 2016. p. 143-331. Section: 3.

[43] Oyen ML. Mechanical characterisation of hydrogel materials. International Materials Reviews. 2014 Jan;59(1):44-59.

[44] Vayron R, Mathieu V, Michel A, Haïat G. Assessment of In Vitro Dental Implant Primary Stability Using an Ultrasonic Method. Ultrasound in Medicine & Biology. 2014 Dec;40(12):2885-94.

[45] Vayron R, Nguyen VH, Lecuelle B, Haiat G. Evaluation of dental implant stability in bone phantoms: Comparison between a quantitative ultrasound technique and resonance frequency analysis. Clinical Implant Dentistry and Related Research. 2018 Aug;20(4):470-8.

[46] Ringleb SI, Chen Q, Lake DS, Manduca A, Ehman RL, An KN. Quantitative shear wave magnetic resonance elastography: Comparison to a dynamic shear material test. Magnetic Resonance in Medicine. 2005;53(5):1197-201.

[47] Lan G, Singh M, Larin K, Twa M. Common-path phase-sensitive optical coherence tomography provides enhanced phase stability and detection sensitivity for dynamic elastography. Biomedical Optics Express. 2017 Nov;8:5253.

[48] Kennedy KM, Chin L, McLaughlin RA, Latham B, Saunders CM, Sampson DD, et al. Quantitative microelastography: imaging of tissue elasticity using compression optical coherence elastography. Scientific Reports. 2015 Oct;5(1):15538.

[49] Manickam K, Machireddy RR, Seshadri S. Study of ultrasound stiffness imaging methods using tissue mimicking phantoms. Ultrasonics. 2014 Feb;54(2):621-31.

[50] Browne JE, Ramnarine KV, Watson AJ, Hoskins PR. Assessment of the acoustic properties of common tissue-mimicking test phantoms. Ultrasound in Medicine & Biology. 2003 Jul;29(7):1053-60.